Rock magnetic and geochemical record in a sediment core from the eastern Arabian Sea: diagenetic and environmental implications during the late Quaternary

Venigalla Purnachandra Rao[a], Pratima Mohan Kessarkar[a], Shiva Kumar Patil[b], Syed Masood Ahmad[c]

[a] *National Institute of Oceanography, Dona Paula – 403 004, Goa, India*

(E-Mail: vprao@nio.org)

[b] *Indian Institute of Geomagnetism, Alibagh- 402 201, Maharashtra, India*

[c] *National Geophysical Research Institute, Uppal Road, Hyderabad, India*

Abstract

Rock magnetic concentration, grain size and mineralogy parameters together with organic carbon, calcium carbonate, redox-sensitive elements, $\delta^{18}O$ of '*Globigerinoides ruber*' and radiocarbon dating were carried out on a 445 cm long sediment core collected at 1380 m depth off Mangalore, southwestern margin of India. The top 290 cm sediments of the core correspond to the last 18 kaBP. The $\delta^{18}O$ and magnetic records exhibit major events at ~16 kaBP, 14.5 kaBP, 11.5 kaBP and 9.8/8.6 kaBP related to start and intensity of the summer monsoon and climate change, and are synchronous with that of the western Arabian Sea and North Atlantic. The sediments with high magnetic susceptibility correlate with high sedimentation rates. The sediments are dominated by fine-grained magnetite, but those at intervals of 1.2 - 3.8 kaBP and 10 - 13.5 kaBP were subjected to diagenetic changes and resulted in the dissolution of fine-grained magnetites and enrichment of redox-sensitive trace elements (Cu, Ni, Zn, V, Mo and U). The sediments between 290 cm and 445 cm correspond to 18-27 kaBP and are characterized by distinct decrease in magnetic concentration, grain size and mineralogy parameters, high organic carbon, low concentrations of redox-sensitive trace elements and abundant pyritized tubules. In other words, the greater reductive diagenetic conditions indicated by rock-magnetic properties are in contrast with the weak sub-oxic conditions revealed by low concentrations of trace elements in the sediments. The seasonal organic matter flux produced during the winter monsoon and moderate sedimentation rates favoured reductive diagenesis in the late glacial sediments. Intermittent bioturbation, however, allowed oxidants to penetrate into the sediments, remobilized redox-sensitive trace elements to the water column and modified the primary geochemical signal of the sedimentary environment.

Keywords: Rock magnetic properties, trace metals, reductive diagenesis, sedimentary environment, late Quaternary, SW margin of India

1. Introduction

A high resolution magnetic study of the sediments offers valuable information in three different domains: (a) Magnetic properties of the sediments respond to paleoclimatic influences which cause changes in sediment source and in the ratio of biogenic to terrigenous sedimentary components (Robinson, 1986; Bloemendal et al., 1993). (b) Magnetic properties are sensitive to detect authigenic magnetite and ultra-fine magnetite formed by bacteria (Kirschvink and Chang, 1984; Karlin et al., 1987; Stolz et al., 1990). (c) Rock-magnetic measurements can also be used to understand the sedimentary environment as magnetic minerals are diagenetically altered in the presence of sub-oxic to anoxic bottom / pore water conditions and/or organic matter (Karlin and Levi, 1983; Leslie et al., 1990; Robinson, 1990). The intensity of diagenesis or post-depositional evolution of sediments depends upon their organic matter content, sedimentation rate, bottom water oxygenation and degree of mixing in the upper sediment layer (Canfield and Berner, 1987; Robinson and Sahota, 2000; Rey et al., 2005). These sediment features will ultimately determine whether or not suboxic/anoxic conditions become established in the sediment. Therefore, understanding the impact of early diagenesis on magnetic minerals has been important for interpreting the sedimentary environment (Snowball and Thompson, 1990; Verosub and Roberts, 1995).

On the other hand, sediments beneath the coastal upwelling areas are known to accumulate considerable amounts of bio/redox-sensitive trace elements which tend to be more soluble under oxidizing conditions and less soluble under reducing conditions. Trace elements such as Cu, Ni and Zn are usually associated with organic matter and may be retained with pyrite even after organic matter is decayed in reducing sediments (Calvert and Pederson, 1993). The elements U, V and Mo originate from an early diagenetic source and enter the sediment via diffusion from the water column. They enrich in sub-oxic environments and strongly enrich in anoxic-euxinic conditions (Brumsack, 2006). The concentrations of Mn strongly deplete in reducing conditions and enrich in oxidizing conditions (Boning et al., 2004). The authigenic enrichment / depletion of redox-sensitive trace metals are thus useful in distinguishing the depositional environment, though caution needs to be exercised in areas of low sedimentation rates and bio-turbation (Calvert and Pederson, 1993; Boning et al., 2004; Brumsack, 2006; Tribovillard et al., 2006; McKay et al., 2007). The objective of this paper is to document variations of rock-magnetic properties and redox-sensitive trace elements in a gravity core obtained off Mangalore, southwestern margin of India (Eastern Arabian Sea) and report changes in diagenesis and sedimentary environment during the late Quaternary.

2. Oceanographic setting

The Arabian Sea experiences seasonal reversal of monsoonal winds that are responsible for changes in hydrography and upwelling-induced biological productivity in the region. The SW (summer) monsoon is more intense in the Arabian Sea and causes high biological productivity, which in turn is responsible for the formation of mid-water oxygen minimum zone (OMZ). The present day OMZ impinges the continental margins at depths between 150 and 1200 m (Qasim, 1982) and also in open northern Arabian Sea (Rostek et al., 1997). The sedimentary records of the western, northern and eastern Arabian Sea exhibit significant variations in productivity and temporal variability of the OMZ, including weakened or non-existent OMZ or intense OMZ conditions during both the glacial and interglacial timescale intervals (Rostek et al., 1993, Cayre and Bard, 1999; Schulte et al., 1999; Reichart et al., 2002; Pattan et al., 2003). The depth (1380 m) at which the core was collected lies within an oxygenated zone below the present-day depth of the OMZ. During the Last Glacial Maximum (LGM) SW monsoon was weaker and NE (winter) monsoon was stronger both in the northern and southeastern Arabian Sea (Rostek et al., 1997; Reichart et al., 2002). Stronger winter monsoon winds induce deepening of surface mixed layer and injection of nutrients to the euphotic zone leading to enhanced productivity in surface water and high organic matter to the bottom sediments.

3. Materials and Methods

During the 63rd cruise of *A A Sidorenko* a 4.45 m long sediment gravity core was recovered at 1380 m depth off Mangalore, southwestern margin of India (Fig. 1). The sediments throughout the core are olive grey, silty clay / clayey silts. The core was sectioned onboard at 2 cm interval for the top 1 m and 5 cm for the rest of the core. Subsamples were oven dried at <40° C. Magnetic measurements on the samples were made using a Barrington MS-2 magnetic susceptibility meter (with an AC magnetic field amplitude of 80 A/m) linked to a MS2B dual frequency sensor (470 and 4700 Hz) at the Indian Institute of Geomagnetism (IIG), Alibagh, India. Representative samples were packed into 8 cm^3 styren cubic pots. Low-frequency (0.47 kHz) magnetic susceptibility (χ_{lf}) was measured three times on each sample and presented as mass specific values in 10^{-8} m^3/kg SI units. The χ_{lf} mainly reflects changes in the concentration of magnetic minerals (Thompson and Oldfield, 1986). Anhysteretic Remnant magnetization (ARM) was imparted to the samples by superposing a DC biasing field of 0.05 mT on a smoothly decreasing alternating field with a peak of 100 mT. It is customary to express ARM as an anhysteretic susceptibility χ_{ARM} (mass specific ARM/strength of the biasing field). χ_{ARM} is sensitive to the concentration of stable single domain (SSD) and pseudo-single domain (PSD) ferrimagnetic grains (Oldfield, 1991). Isothermal Remnant Magnetization (IRM) acquisition was carried out using a Molspin Pulse Magnetizer and remanences were measured by Molspin spinner magnetometer. Saturation Isothermal Remanent Magnetization (SIRM) was imparted using a maximum field of 1 T. After acquisition of SIRM, the samples were subjected to reverse DC fields of 0.3 T and the remanence was measured by using the Molspin magnetometer. SIRM responds primarily to the concentration of ferrimagnetic material, but unlike χ_{lf} it is not affected by diamagnetic and paramagnetic minerals. The interparametric ratios of χ_{ARM}/χ_{lf}, χ_{ARM}/SIRM vary inversely with magnetic grain size and are used to asses the relative change in the concentrations of fine magnetic grain sizes (Maher, 1988). S-ratios ($S_{-0.3T}$) are calculated using the definition of Robinson (1986) and Bloemendal et al. (1988). The S-ratio reflects variations in the coercivity spectrum of magnetic mineral assemblage and therefore mineralogy.

The organic carbon content of the sediments was determined using CNS analyser (NCS 2500). The reproducibility values of organic carbon are better than ±1%. The $CaCO_3$ content was measured using a coulometer. Reproducibility of the measurements was found to be better than ±5%. Planktonic foraminifer '*Globigerinoides ruber*' was picked up from the sediments and $\delta^{18}O$ analyses of the foraminifer were carried out using GV Isoprime Mass Spectrometer facility at the National Institute of Oceanography (NIO), Goa. The analytical standard deviation based on replicates of laboratory standards was better than ±0.07‰. Accelerator Mass Spectrometer (AMS) ages were measured on the same foraminifer picked up from five sediment intervals, using NOSAMS facility at Woods Hole, USA. The radiocarbon ages were calibrated to calendar ages using calib 5.0.2 (Stuiver et al., 2005) and CalPal online software (http://www.calpal-online.de) and calendar ages are discussed through out the study (Table 1). Major elements such as Fe, Mn, Al and several others (not discussed here) were analyzed for the sediment samples of different intervals by ICP-AES at NIO, Goa. Trace element concentrations were determined on different samples using ICP-MS at the National Geophysical Research Institute, Hyderabad, following the method described by Govindaraju (1994). The Al-normalized enrichment factors (ANEFs) of trace elements with respect to the composition of PAAS (Taylor and McLannan, 1985) are calculated (see Table 2).

4. Results

4.1. Chronology and sedimentation rates

The core represents a period for the last 27.1 kaBP. The sediments at the core top are not dated as the top few centimeters of sediments in the gravity core are slided. It is unknown the core top represents 0 kyrs. The age of the sediments between 18 and 22 cm is 1.2 kaBP. The depth vs. age plot of the sediments, shown in Fig. 2, indicates that the rates of sedimentation vary between 8 cm/kyr and 29 cm/kyr. The age model seems to suggest higher rates of sedimentation for the sediments older than 11.5 kaBP and lower rates for those younger than 11.5 kaBP.

4.2. Variations in $\delta^{18}O$, χ_{lf}, Fe, organic carbon and $CaCO_3$ (Fig. 3)

The $\delta^{18}O$ record of '*G. ruber*' indicates that the heavier $\delta^{18}O$ values, characteristic of the late glacial sediments are continued until 16 kaBP. The $\delta^{18}O$ excursion to lighter values is a two step event, between 16 kaBP and 13 kaBP and between ~11.8 kaBP and until late Holocene, interrupted by heavier $\delta^{18}O$ values between 13 kaBP and 11.8 kaBP that correspond to Younger Dryas (YD; see Fig. 3). The glacial and interglacial amplitude in $\Delta\delta^{18}O$ values is ~2.1‰. The χ_{lf} values range from 10 SI units to 50 SI units for the last 17 ka sediments, decrease dramatically to low values (up to 8 SI units) for the sediments between 17 kaBP and 18 kaBP and continued to be low until 27 kaBP. The total iron content varies from 2.8 to 5.4%. Down core distribution of total Fe is parallel to that of χ_{lf} for the last 17 ka sediments but differs distinctly with χ_{lf} below 18 ka (Fig. 3). The distribution of Mn is similar to that of Fe. Organic carbon (OC) is in general roughly reverse to that of χ_{lf} for the last 17 ka sediments. The OC is ~4.5% close to the core top, decreases down core gradually to a minimum of ~1.1% between 11.5 kaBP and 9 kaBP and then increases gradually to 2.8% towards the late glacial sediments. It is ~2.5% between 18 and 27 kaBP. The down core distribution of $CaCO_3$ mimics that of OC (Fig. 3).

4.3. Rock magnetic properties (Fig. 4)

For convenience of description of magnetic parameters the core is divided into section A (0 - 290 cm) and section B (290 - 445 cm). Section A is further subdivided into five intervals, as shown in Fig. 4. S-ratios (0.9 - 0.98) do not show much variations within section A. The χ_{lf}, χ_{ARM} and SIRM values in intervals 1, 3 and 5 are higher and are accompanied by high χ_{ARM}/χ_{lf} and

χ_{ARM}/SIRM ratios. In the interval 5, the increase in χ_{ARM}/χ_{lf} and χ_{ARM}/SIRM ratios is marked with the decrease in OC values. In the interval 3 the χ_{lf} values are peaked at 9.8 and 8.6 kaBP and then decrease gradually upward with a proportional increase in χ_{ARM}/χ_{lf}, χ_{ARM}/SIRM ratios and OC. SIRM/χ_{lf} fluctuates between 6 and 14 kA/m. The sediments in interval 2 exhibit a distinct trough of low magnetic concentration (χ_{lf}, χ_{ARM}, SIRM) and grain size (χ_{ARM}/χ_{lf}, χ_{ARM}/SIRM and SIRM/χ_{lf}) parameters and high OC. In the interval 4 OC values are the least. The χ_{lf} and SIRM values continued to be high, but χ_{ARM} and ARM numerator based ratios (χ_{ARM}/χ_{lf}, χ_{ARM}/SIRM) show a minor trough of low values in this interval (see arrows in Fig. 4). In contrast to section A, all rock magnetic parameters (concentration, grain size and mineralogy) decrease sharply to low values in section B. The OC values are relatively high in this section. S-ratios increase marginally near to the end of section B (Fig. 4).

4.4. Coarse fraction constituents

The >125 μm fraction of the sediments is dominated by planktonic foraminifers through out the core. Keels (dissoluted fragments of planktonic foraminifers) constitute up to 40% in the upper 46 cm of the core. Pyrite occurs as traces to <5% in the sediments of section A, but becomes an important constituent (24 to 35%) in section B. Pyritized grains occur largely as elongated tubules (Fig. 5), platy particles and molds of echinoid spines.

4.5. Trace elements (Fig. 6)

The concentrations of Mn and V are lower and U and Mo higher than that of shale through out the core. The concentrations of Cu, Ni and Zn however fluctuate slightly above and below that of shale. The Al-normalized profiles of Cu, Ni, Zn, Mo and U exhibit relatively low values of the metals in section B and gradually enhanced values towards the core top in section A (Fig. 6). Within section A, distinct increase in the concentrations of trace metals coincides with high OC and low rates of sedimentation in interval 2 and, low OC and high rates of sedimentation in interval 4. The Al-normalized enrichment factors (ANEFs) of Mn and V are marginally high in section B than in section A. The ANEFs of Cu, Ni, Zn, U and Mo are low in section B but increase gradually towards the core top in section A (Table 2).

5. Discussion

5.1 Sediments of section A

5.1.1 Monsoonal and climatic events from $\delta^{18}O$ and rock-magnetic records

The glacial-interglacial $\Delta\delta^{18}O$ amplitude of ~2.1‰ is larger than that of the combined global ice volume effect (1.2‰) and regional deglacial warming (0.5‰) (Rostek et al., 1997; Sonzogni et al., 1998). The $\Delta\delta^{18}O$ of ~2‰ was reported by Thamban et al. (2001) and Prabhu et al. (2004) on the eastern Arabian Sea and interpreted that the $\delta^{18}O$ values are influenced by changes in local hydrography such as precipitation caused by the summer monsoon. Sirocko et al. (1996) described four major $\delta^{18}O$ events, started at ~16 kaBP, 14.5 kaBP, 11.6 kaBP and 9.7 kaBP over the North Atlantic, Greenland and western Arabian Sea cores and suggested a close connection between high latitude climate and tropical monsoons. Of these, the 16 kaBP and 11.6 kaBP events (the $\delta^{18}O$ excursion to low values) are distinct in our record (Fig. 3). The event at 14.5 kaBP is considered as the first abrupt deglacial warming event over the North Atlantic and Greenland. In the western Arabian Sea this event was not visible in the $\delta^{18}O$ record, but was reflected in Ba and dust flux records (Sirocko et al., 1996). In Fig. 3, this event is merged with a broad peak of low $\delta^{18}O$ values. The χ_{lf} record, however, exhibits distinct high values at ~14.5 kaBP. Upwelling indicator for monsoon intensity in the western Arabian Sea showed SW monsoon of maximum intensity at ~9.7 kaBP during the Holocene (Sirocko et al., 1996) and between 9 kaBP and 8.5 kaBP in the eastern Arabian Sea (Thamban et al., 2001, 2007). The event at 9.7 kaBP is not well pronounced in $\delta^{18}O$ record but distinct peaks at ~9.8 kaBP and 8.6 kaBP are present in χ_{lf} record (see Fig. 3). Since χ_{lf} reflects the concentration of magnetic material largely associated with terrigenous supply, it can be used as proxy indicator of southwest monsoon strength. Therefore, the events related to summer monsoon and climate change in our $\delta^{18}O$ and magnetic records (eastern Arabian Sea) are synchronous with that of western Arabian Sea and North Atlantic. Gupta et al. (2003) also showed the links between monsoonal variability in the western Arabian Sea and abrupt changes in the North Atlantic climate during the Holocene.

The Younger Dryas (YD) cold event in our records is associated with heavier $\delta^{18}O$ values, peak of high χ_{lf} and high values of total Fe and Mn (Fig. 3). Tang et al. (2003) also reported the enrichment of Fe_2O_3, Mn and χ_{lf} at YD for the sediments of the Western Pacific and suggested that during cold periods the Fe of magnetite is admixed with Mn and forms $MnFe_2O_4$.

5.1.2 Magnetic materials in intervals 5, 3 and 1

High χ_{ARM}/χ_{lf}, χ_{ARM}/SIRM ratios and high S-ratios indicate fine-grained, low-coercivity minerals (magnetite or titano-magnetite) are dominant at these intervals. The SIRM/χ_{lf} ratios of 6 and 14 kA/m support ferrimagnetic (titano-) magnetite (see Peters and Dekkers, 2003). The high χ_{lf} values in interval 5 are associated with high sedimentation rates. Moreover, the sharp increase in χ_{lf} which began at ~18 kaBP (Fig. 3) predates the change in δ^{18}O values at ~16 kaBP which is related to the onset of summer monsoon. The high χ_{lf} values are therefore interpreted to be due to high sedimentation rates resulting from winnowing of sediments from the upper slope and, subsequent addition of monsoon-derived detrital flux.

The gradual decrease in χ_{lf} correlates with increase in OC and carbonate (productivity indicators) in interval 3 could imply that the magnetic material is diluted by diamagnetic and biogenic material. The increase in fine-grained magnetite (increase in χ_{ARM}/χ_{lf}, χ_{ARM}/SIRM) is marked with increase in OC (Fig. 4) and decrease in terrigenous material (indicated by decrease in acid-insoluble residue - not shown here); this may indicates that some of the magnetite may have formed *in situ* and thus could be authigenic or biogenic origin. Ultra fine-grained magnetites (<1 μm) are usually contributed by authigenic and biogenic magnetites, formed by magnetotactic bacteria (Ozdemir and Banerjee, 1982; Maher, 1988; Hounslow and Maher, 1999). They suggested that these magnetites are present only in minor quantities and do not make a major contribution to the bulk magnetic properties of the sediments. However, they contribute preferentially to ARM because of their sub-micron size.

5.1.3. Early diagenesis in intervals 4 and 2

High S-ratios at these intervals indicate ferrimagnetic material is the dominant component. The decrease in χ_{ARM} and, χ_{ARM}/χ_{lf} and χ_{ARM}/SIRM (Fig. 4) indicates that the fine-grained ferrimagnetic components are selectively dissolved during early diagenesis at both the intervals (see Karlin et al., 1990). The sediments at interval 2 also exhibit a trough of low values in SIRM and SIRM/χ_{lf} . SIRM is not affected by diamagnetic and paramagnetic minerals but decreases in value with an increase in the concentration of coarse magnetic grains. Therefore, the trough of low values in magnetic concentration and grain size parameters in interval 2 (Fig. 4) indicates dissolution of both bacterial and lithogenic fine-grained magnetites during early diagenesis, leaving a residue of coarse-grained lithogenic magnetites. Abundant keels in interval 2 support dissolution of carbonates in sub-oxic conditions. The post-depositional evolution (degree of diagenetic changes) of sediments in interval 2 is greater than in interval 4; this could be due to the fact that the former are associated with high OC and low sedimentation rates and the latter with low OC and high sedimentation rates.

5.2 Sediments of section B: Abrupt magnetic changes

A sharp decrease in all magnetic parameters in section B indicates that the magnetic mineral assemblages in the sediments were affected greatly by reductive diagenesis. The 24 to 35% of pyritized grains support the arguments that reductive diagenesis strongly affected the magnetic components in such a way that all detrital PSD magnetite dissolved and transformed to pyrite. The depth at which reductive diagenesis begins in the sediments depends on the availability of oxidants, sediment accumulation rates and organic matter. Reductive diagenesis was reported in different environments, i.e., the continental margins with high rates of sedimentation and organic productivity (Bloemendal et al., 1992; Robinson, 1990; Kumar et al., 2005), partially restricted sedimentary basins such as Sea of Japan (Vigliotti, 1997), anoxic sediments from the California continental borderland (Leslie et al., 1990) and abyssal plains with organic-rich turbidite sediments (Sahota et al., 1995). Similarly, reductive diagenesis occurs at different depths in sediment cores from the World Ocean. For example, it was reported at 0.5 m and 0.8 m in two cores from the continental shelf of Korea (Liu et al., 2004), 1.2 to 1.6 m in a core from Japan Sea (Hayashida et al., 2007), 2.35 m from the Yellow Sea (Liu et al., 2005), 7 m in a core from the Northwestern Arabian Sea (Bloemendal et al., 1992), 9.8 m in a core from the Bay of Bengal (Haiyan et al., 2006) and >20 m in a core from the Mascarene plateau (Robinson, 1990). In the core investigated here reductive diagenesis occurs at >2.9 m in the sediments (Fig. 4) which deposited at 16 mm/kyr (Fig. 2). Early diagenesis of varied intensity also occurs in this core at 0.2 -0.42 m and 1.0-1.8 m sediments deposited at 8 cm/kyr and 29 cm/kyr, respectively (Fig. 4). Therefore, sedimentation rate alone is not a determinant factor for the post-depositional diagenetic changes.

The OC content is relatively high in section B. High OC in the late glacial sediments of the eastern Arabian Sea was interpreted to be due to enhanced productivity caused by the stronger winter (NE) monsoon winds and associated convective mixing and mixed layer deepening (Rostek et al., 1993; Singh et al., 2006; Kessarkar and Rao, 2007) or, preservation under reducing conditions (Agnihotri et al., 2003). Pyritized tubules (Fig. 5), however, indicate burrowing activity and prevalence of bioturbated, oxic conditions in these sediments. As high organic flux to the sea floor influences the oxygen content of the bottom water, it appears that the development of sub-oxic to anoxic or reductive diagenetic conditions in the eastern Arabian Sea is largely influenced seasonal influx of organic matter induced by productivity and sedimentation rates.

5.3. Sedimentary environment through redox-sensitive trace elements

5.3.1. Sediments of Section B: The Al-normalized enrichment factors (ANEFs) of U, Mo, Cu, Ni and Zn in section B vary only between 1.25 and 2.99 and are significantly lower than in section A (Table 2; Fig. 6). A value of ANEF ≤ 2 can be considered to be of natural origin and a value >2 is suggestive of enrichment either diagenetic changes or anthropogenic involvement. The low enrichments of metals are in contrast with the results obtained by rock magnetic properties and pyrite content (24-35%) in the coarse fraction, which suggest strong reductive diagenesis in the sediments. The low enrichments of the metals are interpreted to be due to either or a combination of two factors: either fully anoxic bottom water conditions have not been established during the late glaciation, or, after developing sedimentary reducing conditions oxidants were replenished from the overlying water column that resulted in remobilization of some of the redox-sensitive trace metals to the water column (see Zheng et al., 2002; McManus et al., 2005). Oxygenated bottom water conditions were reported during the LGM in the eastern Arabian Sea (Kessarkar et al., 2002; Banakar et al., 2005). The late glacial sediments of the core are organic-rich, deposited at 16 mm/kyr and show evidence of bioturbation. Since winter monsoon is stronger during the LGM, productivity and in turn organic matter flux to the seafloor is seasonal. As a consequence sedimentary redox conditions fluctuate periodically and trace elements get accumulated during reducing conditions. Bioturbation allows penetration of oxidants into the sediments and as a result some of the redox-sensitive trace elements will remobilize into water column. McKay et al. (2007) showed that low sedimentation rates and bioturbation / bioirregation allow a small flux of oxidants from the overlying water column and remobilization of some redox-sensitive elements to the water column. Dean et al. (1997) and Zheng et al. (2002) showed that glacial-interglacial changes in productivity and bioturbation can cause abrupt changes in redox-sensitive elements. We therefore suggest that low concentrations of trace elements were due to their remobilization upon subsequent oxidation during bioturbation.

5.3.2. Sediments of section A: The core was recovered from oxygenated waters below OMZ. The Al-normalized trace elements (Mo, U, Cu, Ni and Zn) and their enrichment factors (Table 2), however, increase gradually towards the core top in section A. The increasing trend of these elements is marked with decreasing OC in intervals 4 and 5 and increasing OC in intervals 1-3 (Fig. 6) suggesting that OC alone is not the sole factor for their distribution. Distinct high values of trace elements in intervals 2 and 4 (Fig. 6) indicate development of diagenetic fronts. In interval 2 high values of trace elements correspond with high OC, low sedimentation rates and intense reducing conditions (indicated by magnetic parameters), whereas in interval 4 with low OC, high sedimentation rates and sub-oxic diagenetic conditions. Therefore, the authigenic enrichment of redox-sensitive trace elements and/or development of post-depositional diagenetic changes in the sediments are governed by the delicate balance between periodic organic supply and sedimentation rates.

6. Conclusions

The sediments of the top 290 cm of the gravity core correspond to the last 18 ka. The $\delta^{18}O$ and χ_{lf} records exhibit major events related to the start and intensity of the summer monsoon and climate change. Fine-grained magnetite is the dominant mineral. However, the early diagenetic changes at 20-42 cm and 102 - 180 cm of the core were resulted in the loss of fine-grained magnetites and enrichment of trace metals. The sediments between 290 and 445 cm correspond to 18-27 kaBP and exhibit strong reductive diagenesis indicated by rock magnetic properties and weak sub-oxic conditions revealed by the low concentrations of redox-sensitive trace elements. The contrasting magnetic and geochemical signatures in this portion of the core are attributed to the influence of seasonal organic flux, moderate sedimentation rates and intermittent bioturbation. Apparently after development of reducing conditions oxidants were introduced into the sediments by bioturbation which resulted in remobilization of trace elements to the water column and modified the geochemical signature of the sedimentary environment.

Acknowledgements

Part of the work was done under DST Young Scientist Project awarded to Dr. Pratima M. Kessarkar. Drs. V.K.Banakar and C. Prakash Babu helped us with geochemical analyses. We thank the Editor and anonymous reviewers for their critical and constructive comments on our manuscript. This is NIO contribution

References

Agnihotri, R., Sarin, M.M., Somayajulu, B.L.K., Jull, A.J.T., Burr, G.S., 2003, Late Quaternary biogenic productivity and organic carbon deposition in the eastern Arabian Sea. Palaeogeography. Palaeoclimatology. Palaeoecology, 197, 43-60.

Banakar, V.K., Oba, T., Chodankar, A.R., Kuramoto, T., Yamamoto, M. and Minagawa, M., 2005. Monsoon related changes in sea surface productivity and water column denitrification in the Eastern Arabian Sea during the last Glacial cycle. Marine Geology, 219, 99-108.

Bloemendal, J., Lamb, B., King, J.W., 1988. Palaeoenvironmental implications of rock-magnetic properties of late Quaternary sediment cores from the eastern equatorial Atlantic. Palaeocenography, 3, 61-87.

Bloemendal, J., King, J.W. Hall, F.R.,Doh, S.J., 1992. Rock-magnetism of late Neogene and Pleistocene deep-sea sediments: relationship of sediment source, diagenetic processes and sediment lithology. Journal of Geophysical Research, 97, 4361-4375.

Bloemendal, J., King, J.W., Hunt, A. et al., 1993. Origin of sedimentary magnetic record at Ocean Drilling Program sites on the Owen Ridge, Western Arabian Sea. Journal of Geophysical Research, 98, 4199-4219.

Boning, O., Brumsack, Hans-J., Bottcher, M.E., Schnetger, B., Kriete, C., Kallmayer, J., Borchers, S.L., 2004. Geochemistry of Peruvian nearsurface sediments. Geochimica et Cosmochimica Acta, 68, 4429-4451.

Brumsack, Hans-J., 2006. The trace metal content of recent organic carbon-rich sediments: Implications for Cretaceous black shale formation. Palaeogeography. Palaeoclimatology. Palaeoecology, 232, 344- 361.

Calvert, S.E., Pedersen T.F., 1993. Geochemistry of recent oxic and anoxic sediments: implications for geochemical record. Marine Geology, 113. 67-88.

Canfield, D.E., Berner, R.A., 1987, Dissolution and pyritization of magnetite in anoxic marine sediments. Geochimica et Cosmochimica Acta, 51, 645-659.

Cayre, O., Bard, E., 1999. Planktonic foraminiferal and alkenone records of the last deglaciation from the eastern Arabian Sea. Quaternary Research, 52, 337-342.

Dean, W.E., Gardner, J.V., Piper, D.Z., 1997. Inorganic geochemical indicators of glacial – interglacial changes in productivity and anoxia on the California continental margin. Geochimica et Cosmochimica Acta, 61, 4507-4518.

Govindaraju, K., 1994. Compilation of working values and sample description for 383 geostandards. Geostandard Newsletter, 18, (special issue) 158 pp.

Gupta, A.K., Anderson, D.M., Overpeck, J.T., 2003. Abrupt changes in the Asian SW monsoon during the Holocene and their links to the North Atlantic Ocean. Nature, 421, 354-356.

Haiyan, L., Shihong, S., Nianqiao, F., Hongqiang, W., 2006. Magnetic records of core MS77-181 in the Bay of Bengal and their paleoenvironmental implications. Chinese Science Bulletin, 51, 1884-1893.

Hayashida, A., Hattori, So., Oda, H. 2007. Diagenetic modification of magnetic properties observed in the piston core (MD01-2407) from the Oki Ridge, Japan Sea. Palaeogeography. Palaeoclimatology. Palaeoecology, 247, 65-73.

Hounslow, M.W., Maher, B.A., 1999, Source of the climate signal recorded by magnetic susceptibility variations in Indian Ocean Sediments. Journal of Geophysical Research, 104, B3, 5047-5061.

Karlin, R., 1990. Magnetic diagenesis in marine sediments from the Oregon continental margin. Journal of Geophysical Research, 95, 4405-4419.

Karlin, R., Levi, S., 1983. Diagenesis of magnetic minerals in Recent hemi-pelagic sediments. Nature, 303, 327-330.

Karlin, R., Lyle, M. Heath, G.R., 1987. Authigenic magnetite formation in suboxic marine sediments. Nature, 326, 490-493.

Kessarkar, P.M., Rao, V.P., 2006. Organic carbon in sedimentsof the southwestern margin of India: Influence of productivity and monsoon variability during the Late Quaternary. Journal of Geological Society of India, 69, 42-52.

Kessarkar, P.M., Rao, V.P., Naqvi S.W.A., Groots, P.M. 2002 Fluctuations in productivity and denitrification intensity along the southwestern continental margin of India since the last glacial maximum. EOS Trans. AGU, 83(47), Fall Meet. Suppl., Abstract PP71B-0394.

Kirschvink, J.L., Chang, S.B.R., 1984. Ultrafine-grained magnetite in deep sea sediments. Possible bacterial magnetofossils. Geology, 12, 559-562.

Kumar, A.A., Rao, V.P., Patil, S.K., Kessarkar, P.M., Thamban, M., 2005. Rock magnetic records of the sediments of the eastern Arabian Sea: Evidence for late Quaternary climatic change. Marine Geology, 220, 59-82.

Leslie, B.W., Lund, S.P. and Hammond, D.E. 1990. Rock magnetic evidence for the dissolution and authigenic growth of magnetic minerals within anoxic marine sediments of the California Continental Borderland. Journal of Geophysical Research, 95, 4437-4452.

Liu, J., Zhu, R., Roberts, A.P., Li, S., Chang, J-H., 2004, High-resolution analysis of early diagenetic effects on magnetic minerals in post-middle-Holocene continental shelf sediments from the Korea Strait, Journal of Geophysical Research, 109, B03103, 1-15.

Liu, J., Zhu, R.X., Li, S.Q. et al., 2005. Magnetic mineral diagenesis in the post-glacial muddy sediments from the southeastern South Yellow Sea. Response to marine environmental changes. Science China Series D-Earth Sciences, 48, 134-144.

McKay, J.L., Pedersen, T.F., Mucci, A. 2007. Sedimentary redox conditions in continental margin sediments (N.E.Pacific) – Influence on the accumulation of redox-sensitive trace metals. Chemical Geology, 238, 180-196.

Maher, B.A., 1988. Magnetic properties of some synthetic sub-micron magnetites. Geophysical Journal, 94, 83-96.

McManus, J., Berelson, W.M., Klinkhammer, G.P., Hanmond, D.E., Holm, C., 2005. Authigenic Uranium: relationship to oxygen penetrationdepth and organic carbon rain. Geochimica et Cosmochimica Acta, 69, 95-108.

Oldfield, F. 1991. Environmental magnetism- A personal perspective. Quaternary Science Reviews, 10, 73-85.

Ozdemir, O., Banerjee, S.K., 1982. A preliminary magnetic study of soil samples from west-central Minnesota, Earth Planetary Science Letters, 59, 393-403.

Pattan, J.N., Masuzawa, T., Naidu, P.D., Parthiban, G., Yamamoto, M., 2003. Productivity fluctuations in the southeastern Arabian Sea during the last 140 ka. Palaeogeography. Palaeoclimatology. Palaeoecology, 193, 575-590.

Peters, C., Dekkers, M.J., 2003. parameters as a function of mineralogy, concentration and grain size. Physics, Chemistry of the Earth, 28, 659-667.

Prabhu, C.N., Shankar, R., Anupama, K., Taib, M., Bonnefille, R., Vidal, L., Prasad, S. 2004. A 200 ka palaeoclimatic record deduced from pollen and oxygen isotope analyses of sediment cores from the eastern Arabian Sea. Palaeogeography. Palaeoclimatology. Palaeoecology, 214, 309-321.

Qasim, S.Z., 1982. Oceanography of the northern Arabian Sea. Deep Sea Research, Part A, 29, 1041-1068.

Reichart, G.J., Nortier, J., Versteegh, G., Zachariasse, W.J., 2002 Periodical breakdown of the Arabian Sea oxygen minimum zone caused by deep convective mixing . In: Clift, P.D., et al. (Eds.), The tectonic and Climatic evolution of the Arabian Sea region, Special Publication, Geological Society of London, Vol. 195, pp. 407-419.

Rey, D., Mohamed, K.J., Bernabeu, A., Rubio, B., Vilas, F., 2005. Early diagenesis of magnetic minerals in marine transitional environments: geochemical signatures of hydrodynamic forcing. Marine Geology, 215: 215-236.

Robinson, S.G., 1986. The late Pleistocene palaeoclimatic record of North Atlantic deep-sea ssediments revealed by mineral magnetic measurements. Phys. Earth Planet. Inter., 42, 22-47.

Robinson, S.G. 1990. Application for whole-core magnetic susceptibility measurements: ODP Leg 115 results. Proceedings of the Ocean Drilling Program Scientific Research, 115, 737-771.

Robinson, S.G., Sahota, J.T., 2000. Rock-magnetic characterization of early, redoxomorphic diagenesis in turbiditic sediments from the Madeira Abyssal Plain. Sedimentology, 47, 307-394.

Rostek, F., Bard, E., Beafort, L., Sonzogni, C., Ganssen, G. 1997. Sea surface temperature and productivity record for the past 240 kyrs in the Arabian Sea. Deep-sea Research –II, 44, 1461-1480.

Rostek, F., Rhuland, G.,, Bassinot, F.C., Muler, P.J., Labeyrie, L., Lancelot, Y., Bard, E. 1993. Reconstructing sea surface temperature and salinity using ^{18}O and alkenone records, Nature, 364, 319-321.

Sahota, J.T.S., Robinson, S.G., Oldfield, G. 1995. Magentic measurements used to identify paleoxidation fronts in deep-sea sediments from the Madeira Abyssal Plain. Geophysical Research Letters, 22, 1961-1964.

Schulte, S., Rostek, F., Bard, E., Rulkotter, J., Marchal, O., 1999. Variation of oxygen minimum and primary productivity recorded in sediments of the Arabian Sea. Earth Planetary Science Letters, 173, 205-221.

Singh, A.D., Kroon, D., Ganeshram, R.S., Millennial scale variations in productivity and OMZ intensity in the eastern Arabian Sea. Journal of Geological Society of India, 68, 369-378.

Sirocko, F., Garbe-Schonberg, McIntyre, Molfina, B., 1996. Teleconnections between the subtropical monsoons and high-latitude climates during the last glaciation. Science, 272, 526-529.

Snowball, I.F., Thompson, R., 1990. A stable chemical remanence in Holocene sediments. Journal of Geophysical Research, 95, 4471-4479.

Sonzogni, C., Bard, E., Rostek, F. 1998. Tropical sea surface temperatures during the last glacial period: a view based on alkenones in the Indian ocean sediments. Quaternary Science Reviews, 17, 1185-1201.

Stolz, J.F., Lovley, D.R., Haggerty, S.E., 1990. Biogenic magnetite and the magnetization of sediments. Journal of Geophysical Research, 95, 4355-4361.

Stuiver, M., Reimer, P.J., Reimer, R.W., 2005. CALIB 5.0.2 [Program and documentation]. http://www.calib.qub.ac.uk/.

Tang, X., Chen, Z., Yan, W., Chen, M., 2003. Younger Dryas and Heinrich events recorded by magnetic susceptibility of sediments from the central temperature area of Western Pacific Warm Pool. Chinese Science Bulletin, 48, 808-813.

Taylor, S.R., McLennan, S.M., 1985. Continental crust: its composition and evolution. Blackwell, Oxford, 311 pp.

Thamban, M., Rao, V.P., Schneider, R.R., Grootes, P.M., 2001. Glacial to Holocene fluctuations in hydrography and productivity along the southwestern continental margin of India. Palaeogeography, Palaeoclimatology, Palaeoecology, 165, 113-127.

Thamban, M., Kawahata, H., Rao, V.P., 2007. Indian Summer monsoon variablility during the Holocene as recorded in sediments of the Arabian Sea: Timing and implications. Journal of Oceanography, 63, 1009-1020.

Thompson, R., Oldfield, F. 1986. Environmental magnetism. Allen and Unwin, Boston, Mass.

Tribovillard, N., Algeo, T.J., Lyons, T., Ribaulleau, A. 2006. Trace metals as paleoredox and paleoproductivity proxies: An update. Chemical Geology, 232, 12-32.

Verosub, K.L., Roberts, A.P. 1995. Environmental magnetism: past, present and future. Journal of Geophysical Research, 100, 2175-2192.

Vigliotti, L. 1997 Magnetic properties of light and dark sediment layers from the Japan Sea: diagenetic and paleoclimatic implications. Quaternary Science Reviews, 16, 1093-1114.

Zheng, Y., Anderson, R.F., van Geen, A., Fleishier, M.Q. 2002. Remobilization of authigenic U in marine sediments by bioturbation. Geochimica et Cosmochimica Acta, 66, 1759-1772.

Figure captions

Fig. 1. Location of the gravity core on the western margin of India.

Fig. 2. A plot showing the Depth vs. Age of the sediments in the core. Sedimentation rates for different intervals are also shown.

Fig. 3. Down-core variations of $\delta^{18}O$, $\chi_{lf,}$ total Fe (Fe%), Mn, organic carbon (OC), $CaCO_3$ and linear sedimentation rates (LSR). Horizontal lines are events related to the start and intensity of summer monsoon and climate change and, younger dryas (YD).

Fig. 4. Down-core variations of OC and, rock magnetic concentration, grain size and mineralogy parameters. No's. 1, 2, 3, 4 and 5 are intervals in section A. The actual depth at which the intervals occur in the core and their calibrated ages (in brackets) are also shown.

Fig. 5. Photomicrograph of pyritized tubules in the sediments of section B in the core.

Fig. 6. Down-core variations of Al-normalized ratios of OC, Mn, V, Mo, U, Cu, Ni and Zn.

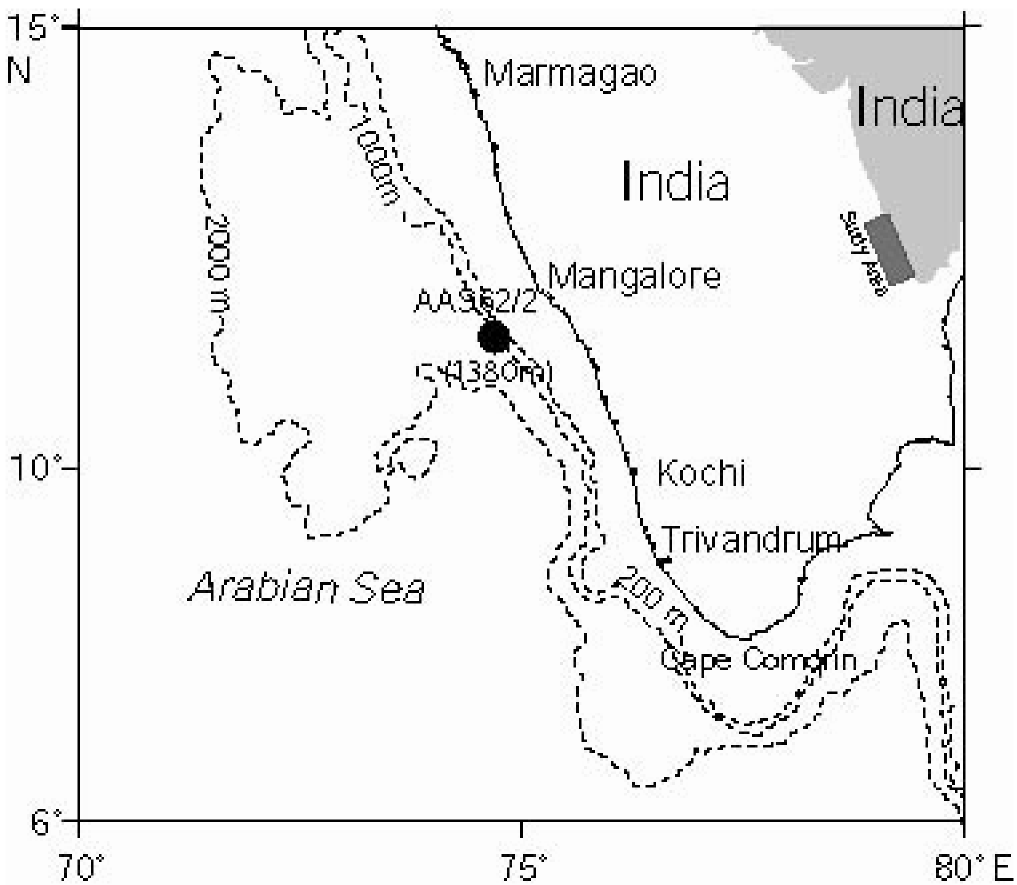
15°
N
Marmagao
India
India
1000m
2000 m
Mangalore
AAS62/2
(1380m)
10°
Kochi
Trivandrum
Arabian Sea
200 m
Cape Comorin
6°
70°
75°
80° E

FIG. 1

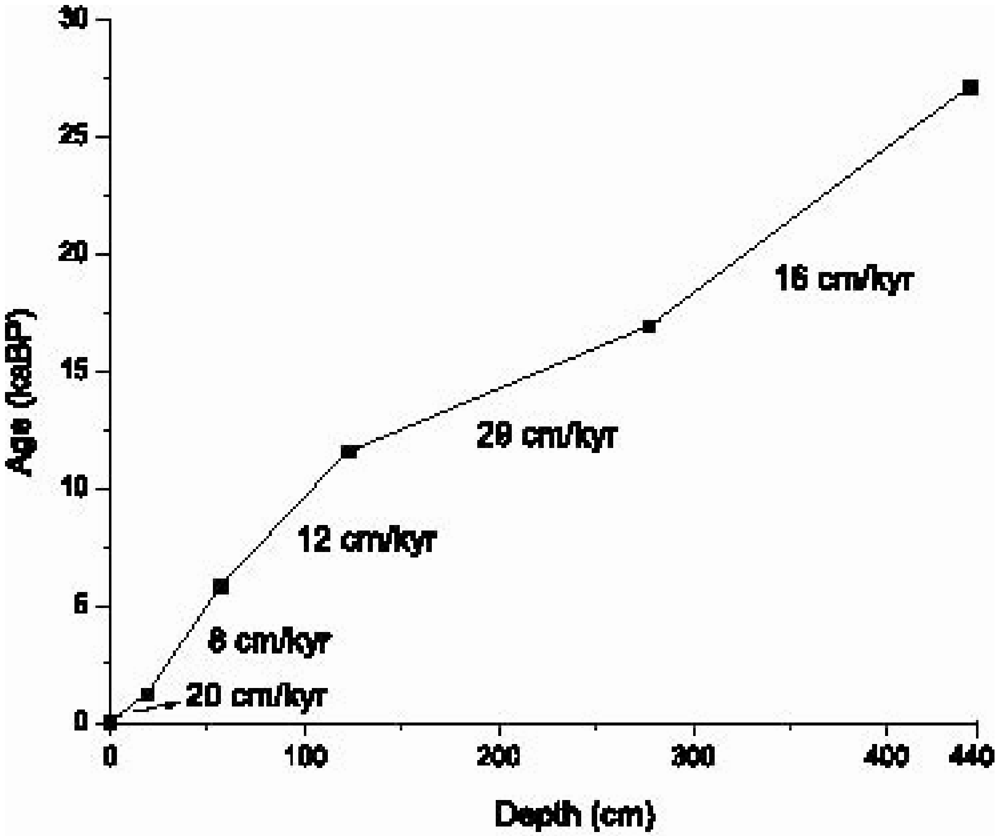

30
25
20
15
10
5
0
Age (kaBP)
16 cm/kyr
29 cm/kyr
12 cm/kyr
8 cm/kyr
20 cm/kyr
0
100
200
300
400
440
Depth (cm)

FIG. 2

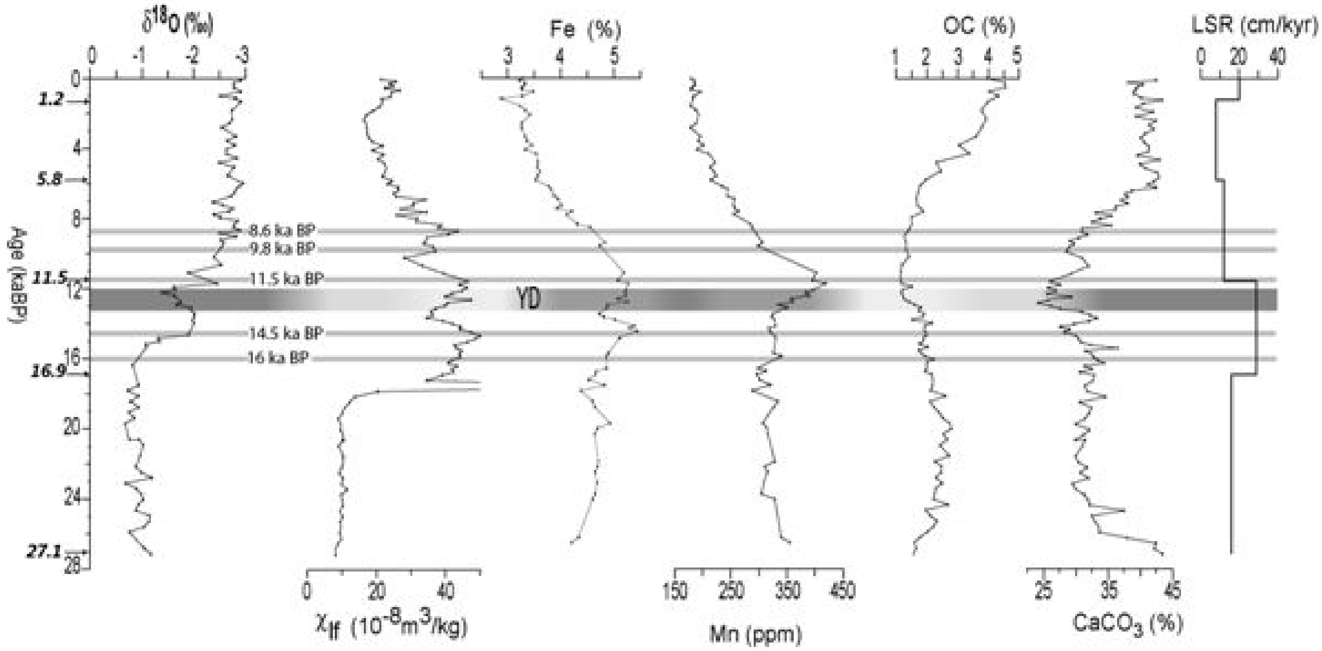

δ18O (‰)
Fe (%)
OC (%)
LSR (cm/kyr)
Age (kaBP)
1.2
5.8
11.5
16.9
27.1
8.6 ka BP
9.8 ka BP
11.5 ka BP
14.5 ka BP
16 ka BP
YD
χlf (10-8m3/kg)
Mn (ppm)
CaCO3 (%)

FIG. 3

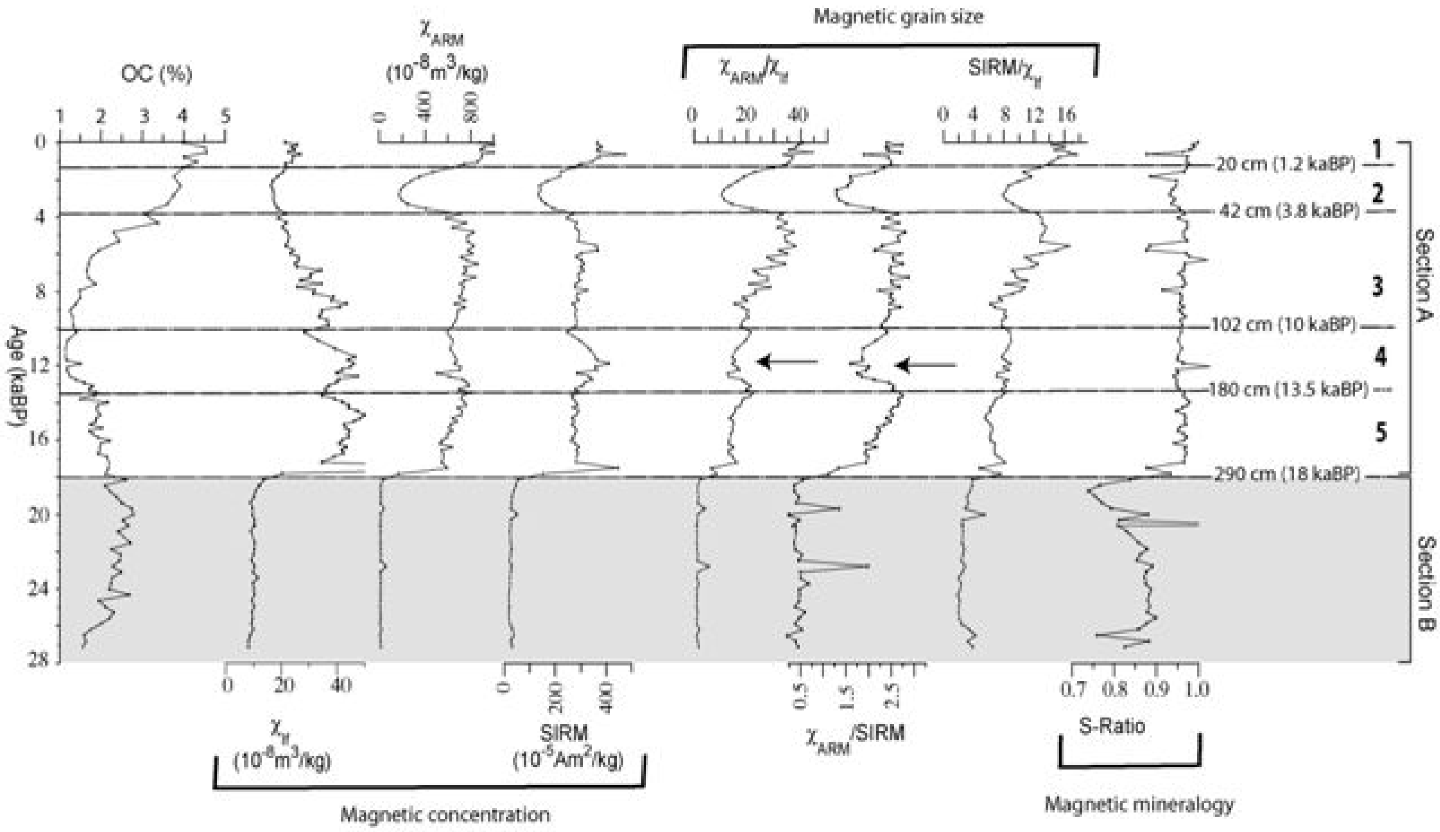

Magnetic grain size
OC (%)
χARM (10-8m3/kg)
χARM/χlf
SIRM/χlf
Age (kaBP)
20 cm (1.2 kaBP)
42 cm (3.8 kaBP)
102 cm (10 kaBP)
180 cm (13.5 kaBP)
290 cm (18 kaBP)
1
2
3
4
5
Section A
Section B
χlf (10-8m3/kg)
SIRM (10-5Am2/kg)
χARM/SIRM
S-Ratio
Magnetic concentration
Magnetic mineralogy

FIG. 4

FIG. 5

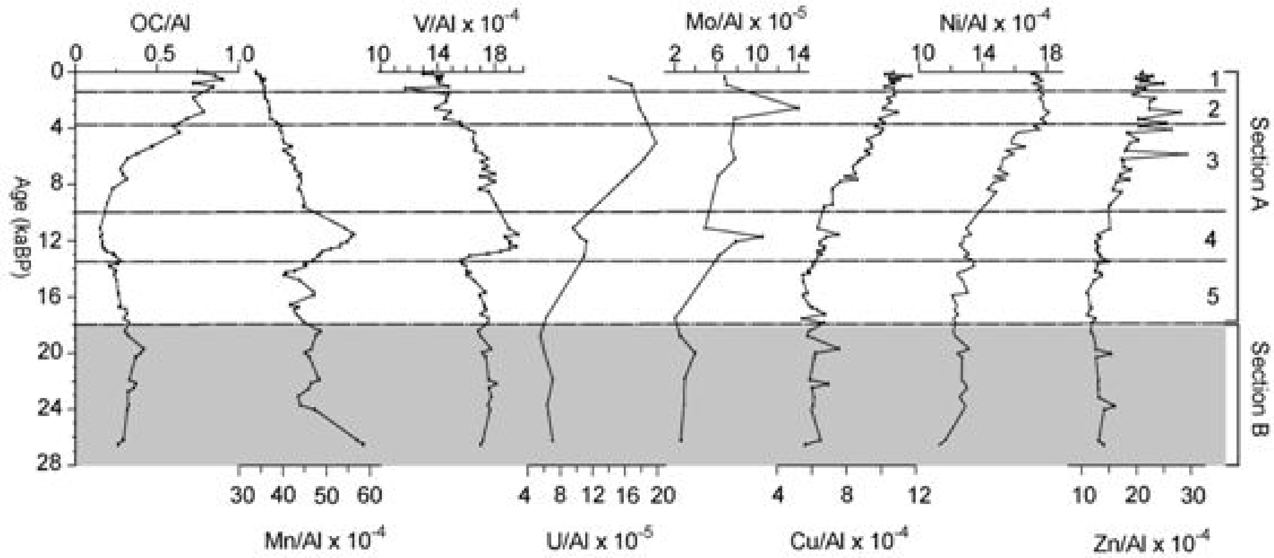
OC/Al
0
0.5
1.0
V/Al x 10-4
10
14
18
Mo/Al x 10-5
2
6
10
14
Ni/Al x 10-4
10
14
18
Age (kaBP)
0
4
8
12
16
20
24
28
1
2
3
4
5
Section A
Section B
30 40 50 60
Mn/Al x 10-4
4 8 12 16 20
U/Al x 10-5
4 8 12
Cu/Al x 10-4
10 20 30
Zn/Al x 10-4

Fig. 6

Table 1. Accelerator Mass Spectrometer (AMS) ages of sediment intervals dated in the core AAS-62/2

Depth interval in the core (cm)	Lab code at WHOI	Radiocarbon Age (years)	Error (± years) 2SD	Calibrated Age (Years)
18-22	50069	1800	100	1205
56-58	50070	5580	55	5798
120-125	50071	10550	60	11542
275-280	50072	14700	70	16894
440-445	54962	22600	120	27093

WHOI- Woods Hole Oceanographic Institution, USA

Table 2: Al-normalized enrichment factors (ANEFs) of trace elements (average) for different intervals in section A and B for the core AAS-62/2 (see Fig. 6 for intervals and sections of the core)

Section	Intervals	Mn	V	Cu	Ni	Zn	U	Mo
Section A	1	0.41* *(0.40-0.42)*#	0.92 (0.78-0.99)	2.15 *(2.00-2.35)*	3.17 *(3.10-3.23)*	2.54 *(2.42-2.94)*	5.00 *(4.57-5.43)*	7.00 *(6.92-7.07)*
(0 - 290 cm)	2	0.44 *(0.42-0.47)*	0.99 *(0.92-1.04)*	2.06 *(2.00-2.19)*	3.22 *(3.13-3.30)*	2.67 *(2.27-3.30)*	5.86 *(5.74-5.97)*	10.99 *(7.86-14.12)*
	3	0.50 *(0.47-0.53)*	1.51 *(1.08-1.21)*	1.71 *(1.30-2.00)*	2.79 *(2.55-3.20)*	2.19 *(1.76-3.11)*	5.85 *(5.24-6.40)*	7.20 *(6.27-7.87)*
	4	0.61 *(0.55-0.66)*	1.22 *(1.04-1.31)*	1.31 *(1.24-1.50)*	2.35 *(2.32-2.46)*	1.57 *(1.47-1.78)*	3.41 *(3.08-3.63)*	7.48 *(4.99-10.61)*
	5	0.51 *(0.48-0.54)*	1.12 *(1.05-1.17)*	1.18 *(1.09-1.35)*	2.29 *(2.19-2.45)*	1.43 *(1.29-1.58)*	2.00 (--)	2.05 (--)
Section B (290 - 445 cm)		0.56 *(0.51-0.69)*	1.16 *(1.12-1.18)*	1.25 *(1.15-1.50)*	2.27 *(2.12-2.36)*	1.56 *(1.38-1.85)*	2.07 *(1.79-2.27)*	2.99 *(2.53-3.98)*

ANEF= $(\text{Element/Al})_{\text{sediment sample}}$ / $(\text{element/Al})_{\text{PAAS}}$; PAAS – Values reported by Taylor and McLennan (1985).

*Average value; # range of value